Bull. Nov. Comp. Center, Num. Anal., 13 (2005), 21–31

On the finite volume approach to the 3D quasistructured grids*

V.P. Il'in, M.V. Pavlov, A.P. Volkov

Abstract. The finite volume methods and technologies for the solution of the 3D elliptic boundary value problems (BVPs), with a complex geometry, on the quasistrucured grids are proposed. The grid data structure and the element-by-element approach for computing the local balance and assembling the global matrices are considered. The results of numerical experiments, obtained with the help of the preconditioned conjugate gradient algorithm, demonstrate the efficiency of the proposed technologies.

1. Introduction

The most widespread approaches to the numerical solution of the BVPs with complicated curvilinear boundary surfaces are finite element methods (FEMs) and finite volume methods (FVMs) (see, e.g., [1, 2]). One of the main technological problems in mathematical modeling is the adapted discretization of a computational domain and the automatic construction of the approximation algorithms. Of course, challenging issue in the 3D BVPs is grid generation for piece-wise smooth boundary and piece-wise smooth coefficients of the partial differential equations (PDEs), i.e., different material properties in subdomains (see [3, 4] and the references therein). A success of this computational step is provided by means of its grid data structure (GridDS) which is usually know-how of the developers of the applied program packages (APPs), for example, see information about ANSYS and FEMLAB in Internet. The second implementation aspect of FVM (or FEM) is element-by-element technology of approximation stage, based on computing the local balance (or local stiffness) matrices and assembling the global matrix.

We use, in fact, a mixed finite volume method which includes the approximation of the density of a substance and its flux simultaneously [8]. In addition to GridDS, an efficient realization of these algorithms for a wide class of BVPs and PDEs needs a careful formalization of the geometrical and functional data structure (Geom and FDS) which must support the description and modification of mathematical objects in the original problems to be solved [5, 6]. The final result of these procedures is algebraic data

*Supported by the Russian Foundation for Basic Research under Grant 05-01-00487 and NWO-RFBR under Grant 047.016.008.

structure (ADS), based on conventional sparse matrix formats [7], which presents all necessary information about SLAE (a system of the linear algebraic equations). The third important part of the computational process is a numerical solution of SLAE which is realized for large 3D problems by iterative sparse solvers and does not directly depend on a grid, geometrical and functional data structures.

The aim of this paper is to consider computational technologies on a quasistructured grid which is presented as union of the subdomains with structured grids. The latter means a set of successive ordered mesh objects: nodes, edges, faces and volume elements, with regular numbering and a possibility of finding the neighbors for each representer. In Section 2, we describe the grid data structures at the macrolevel (subdomains) and at the microlevel (mesh objects). In particular, the special type of grid domain (cylinder in parallelepiped) is constructed. Also, the element-by-element FVM technology for a quasistructured grid is described. Section 3 presents the results of numerical experiments, obtained with the help of the preconditioned conjugate gradient algorithm (the explicit incomplete factorization method — EXIFCG, see [9, 10]).

2. Algorithms and technologies of discretization and approximation

The development of the proposed computational methods and technologies is demonstrated on the numerical solution to the diffusion equation

$$-\nabla(\sigma\nabla u) = f(\vec{x}), \quad \vec{x} \in \Omega \subset R^3, \tag{1}$$

with the piece-wise smooth functions $\sigma(\vec{x})$ and $f(\vec{x})$, in the bounded computational domain whose closure is

$$\overline{\Omega} = \Omega \cup \Gamma, \quad \Gamma = \Gamma^e \cup \Gamma^i, \quad \Gamma^e = \bigcup_{m=1}^{M_e} \Gamma^e_m, \quad \Gamma^i = \bigcup_{m=1}^{M_i} \Gamma^i_m. \tag{2}$$

At different parts of the external boundary $\Gamma^e = \Gamma^{e,D} \cup \Gamma^{e,N}$, the Dirichlet or the Neumann (or the Robin) boundary condition can be given:

$$u|_{\Gamma^{e,D}} = g(\vec{x}), \quad \Big(\alpha(\vec{x})u + \frac{\partial u}{\partial \vec{n}}\Big)\Big|_{\Gamma^{e,N}} = \beta(\vec{x}). \tag{3}$$

Here $\vec{n}$ notes the external normal to $\Gamma^{e,N}$. At the internal boundary Γ^i, consisting of the surfaces with jumps of the functions $\sigma(\vec{x})$ or $f(\vec{x})$, the conjunction conditions

$$\sigma^+ \frac{\partial u}{\partial n}\Big|_{\Gamma^{i,+}} = \sigma^- \frac{\partial u}{\partial n}\Big|_{\Gamma^{i,-}}, \quad u|_{\Gamma^{i,+}} = u|_{\Gamma^{i,-}} \tag{4}$$

hold, which are the direct sequence of original equation (1).

The boundary Γ is supposed to be piece-wise smooth. We also assume that the unknown solution $u(\vec{x})$ possesses smoothness in the open domain Ω, sufficient for validity of the approximations.

2.1. Quasistructured grids and data structure. Let us divide the computational domain into such subdomains

$$\Omega = \bigcup_{l=1}^{\bar{l}} \Omega_l \tag{5}$$

that in each Ω_l the functions $\sigma(\vec{x})$, $f(\vec{x})$ are smooth. We can also define an "external subdomain" as $\Omega_0 = R^3 \setminus \Omega$. The internal boundary segment between the two adjacent subdomains Ω_l, $\Omega_{l'}$ can be denoted by a pair of corresponding indices and defined as intersection of the respective closures:

$$\Gamma^i_{l,l'} = \overline{\Omega}_l \cap \overline{\Omega}_{l'}. \tag{6}$$

As for the external boundary, it can formally be presented in a similar manner:

$$\Gamma^e = \bigcup_l \Gamma^e_{l,0} = \bigcup_l \overline{\Omega}_l \cap \overline{\Omega}_0 = \overline{\Omega} \cap \overline{\Omega}_0, \quad \Gamma^e_{l,0} = \Gamma^e_l. \tag{7}$$

A set of the boundary surface segments $\Gamma^e_{l,l'}$ and $\Gamma^i_{l,l'}$ can also be numbered by one index $m = m(l, l')$, $m = 1, \ldots, \bar{m} = M_i + M_e$, i.e.,

$$\Gamma = \Gamma^e \cup \Gamma^i = \bigcup_{m=1}^{\bar{m}} \Gamma_m. \tag{8}$$

Each pair of the intersecting boundary segment surfaces Γ_m, $\Gamma_{m'}$ forms the boundary edge $R_{m,m'}$, either linear or curvilinear. A set of such edges can be numbered by one index:

$$R_{m,m'} = R_q, \quad q = q(m, m') = 1, \ldots, \bar{q}. \tag{9}$$

Formally, the edge R_q is an open 1D point set, and its closure is

$$\bar{R}_q = R_q \cup P_{q,1} \cup P_{q,2}, \tag{10}$$

where $P_{q,1}$ and $P_{q,2}$ are the beginning and the end vertices of R_q, respectively. A set of all the vertices in $\bar{\Omega}$ we denote as $P = \{P_r,\ r = 1, \ldots, \bar{r}\}$. The closure of the surface segment Γ_m is

$$\overline{\Gamma}_m = \Gamma_m \cup \overline{R}_{m,q} = \Gamma_m \cup R_{m,q} \cup P_{m,r}, \quad q \in \omega_m^{f,e}, \quad r \in \omega_m^{f,p}, \tag{11}$$

where $\omega_m^{f,e}$ and $\omega_m^{f,p}$ denote the set of edges and vertices incident to Γ_m, i.e., they form the boundary of Γ_m.

The total set of subdomains Ω_l, $l = 1, \ldots, \bar{l}$, surface segments Γ_m, $m = 1, \ldots, \bar{m}$, boundary edges R_q, $q = 1, \ldots, \bar{q}$, and vertices P_n, $n = 1, \ldots, \bar{n}$, will be considered as a macrogrid, and its object will be called macroelements, macrofaces, macroedges and macronodes, respectively. The topology of the macrogrid is uniquely defined by a set of own objects and by connections between them. For describing these connections we can introduce, similar to $\omega_m^{f,e}$ and $\omega_m^{f,p}$, the sets of the indices: $\omega_n^{p,\Omega}$, $\omega_n^{p,f}$, and $\omega_n^{p,e}$, i.e., the subsets of the numbers of macroelements, macrofaces and macroedges, respectively, which are incident to the macronode P_n; $\omega_l^{\Omega,f}$, $\omega_l^{\Omega,e}$, and $\omega_l^{\Omega,p}$ being the subsets of the numbers of macrofaces, macroedges and macronodes, which are incident to the macroelement Ω_l.

In addition to the topological information, necessary data for identification of a computational domain contains a geometrical description of the boundary surfaces, i.e., their equations. By means of solution to the systems of such equations, macroedges and macronodes can be defined. If such systems have non-unique solutions, some additional constraints have to be given.

Collection of the information considered presents a geometrical data structure (GeomDS) for BVP. The typical computational domains consist of a set of standard macroelements: parallelepipeds, pyramids, spheres, cylinders and cones, for example, as well as of their intersections. The full descretization procedure of BVP must also include the functional information: what coefficients and right-hand sides of PDE are defined in each subdomain Ω_l, what kind of the boundary condition at each external boundary segment $\Gamma_{m,l}^e$ is given. This functional data structure (FDS) is formulated as related to the GeomDS.

The construction of the adapted grid Ω^h in the complicated computational domain Ω can be implemented by discretization of separate subdomains Ω_l. This procedure includes creating discrete analogues to macroedges, macrofaces, and macroelements which are denoted by R_q^h, Γ_m^h, and Ω_l^h, respectively. We suppose all the macronodes to be included into a macrogrid, i.e., $P_r = P_r^h$. If the macroedge R_q is a linear interval, then let $R_q^h = R_q$. Similarly, if the macroface Γ_m is a linear segment, then define $\Gamma_m^h = \Gamma_m$. But generally, R_q^h (or Γ_m^h) can be an approximation of R_q (or Γ_m). For example, for curvilinear R_q or Γ_m, their discrete analogies R_q or Γ_m^h can be presented by piecewise linear segments.

We have also to remark that a subdomain Ω_l^h, in principle, does not approximate a certain computational subdomain, and the numbers of a grid

and computational subdomains can be different. The motivation for the definition of grid subdomains consists in the possibility of constructing a simple grid data structure. The GridDS is defined as a full, but a minimal, information which is required, together with the GeomDS and the FDS, for implementation of approximation algorithms by the element-by-element technology. It includes the coordinates of nodes, equations of the grid edges and faces, formulas for coefficients of PDE and boundary conditions for each element and its boundary faces.

Similar to a macrogrid, a microgrid (a grid in the sequel) is presented by a set of elementary grid objects: nodes $p^h_{n'}$, edges $r^h_{q'}$, faces $\gamma^h_{m'}$, and elements $e^h_{l'}$. The typical elements are a parallelepiped, a tetrahedron, a prism, etc. These figures can be understood in the topological sense if their edges are curvilinear.

The grid computational domain has the own closure

$$\overline{\Omega}^h = \Omega^h \cup \overline{\Gamma}^h = \Omega^h \cup \Gamma^h \cup R^h \cup P^h, \tag{12}$$

and it can be divided into a set of subdomains:

$$\Omega^h = \left(\bigcup_l \Omega^h_l \right) \cup \overline{\Gamma}^{h,i}, \quad \overline{\Omega}^h = \bigcup_l \overline{\Omega}^h_l, \tag{13}$$

where $\bar{\Gamma}^{h,i}$ is the closure of the grid internal boundary.

The idea of a quasistructured grid consists in the possibility of constructing a simple structured grid in the subdomain Ω^h_l if it has a regular geometrical and(or) a topological structure.

We assume, for simplicity, that grids in the adjacent subdomains Ω^h_l, $\Omega^h_{l'}$ are consistent, i.e., they have the same meshpoints at the joint macrofaces and $\Gamma^h_{l,l'} = \Gamma^h_{l'l}$. According to such a structure, each grid object has a double number: the regional (in Ω^h_l) and the global one.

A structured grid is defined as the one which is generated by regular sets of coordinate surfaces and has simple numbering in such a way that for each its object the adjacent objects can be easily found. For a non-structured grid, objects can be given by the direct enumeration, only.

As a special type of a quasistructured grid, we consider the discretization of the figure "cylinder into parallelepiped" presented in Figure 1.

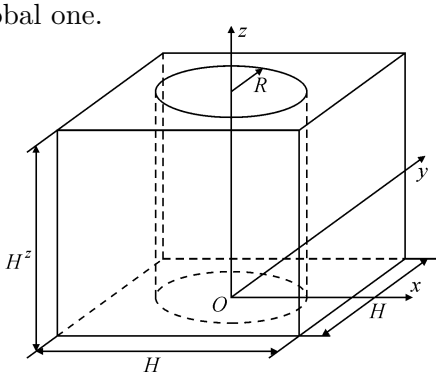

Figure 1. Computational domain "cylinder into parallelepiped"

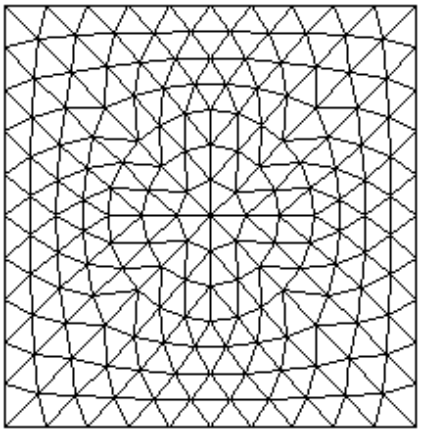

Figure 2. Cross-section of the grid

Here, we have two computational and two grid subdomains. The node Cartesian coordinates of a consistent grid in the cylinder Ω_1 are defined by the simple formulas

$$\begin{aligned} &x_{i,j} = x(r_i, \theta_{j,i}), \quad y_{i,j} = y(r_i, \theta_{j,i}), \\ &z_k = z_0 + kh^z, \quad r_i = ih^r, \\ &\theta_{j,i} = \theta_{j-1,i} + h_i^\theta, \quad h_i^\theta = 2\pi/(3+i). \end{aligned} \tag{14}$$

The grid element in such a case is the triangular prism with one cylindrical face. A sample of grid z-cross-section for Ω_1 and $\Omega_2 = \Omega/\Omega_1$ is described in Figure 2.

2.2. Local and global balance matrices. For the FVM approximation of equation (1), rewrite it in the mixed form

$$\nabla \vec{v} = f(\vec{x}), \tag{15}$$

$$\vec{v} = -\sigma \nabla u, \tag{16}$$

where $\vec{v}$ is a flux vector of the substance.

For the grid node P_n^h define the Dirichlet–Voronoi cell V_n with the surface S_n and the adjacent nodes $P_{n'}^h$, $n' \in \omega_n^{p,p}$. Let $d_{n,n'} = [P_n^h, P_{n'}^h]$ be a line segment and $S_{n,n'}$ be the corresponding cell side, which is perpendicular to $d_{n,n'}$. Let us note that if the node P_n^h is placed at the boundary $\bar{\Gamma}^{e,h}$, then instead of V_n we consider its internal part $V_n \cap \overline{\Omega}^h$, only.

After integration of equations (15), (16) over V_n and $d_{n,n'}$, respectively, we obtain the relations

$$\sum_{n' \in \omega_n^{p,p}} \int\limits_{S_{n,n'}} v_{n,n'}\, ds = \int\limits_{V_n} f(\vec{x})\, dv, \tag{17}$$

$$u_n - u_{n'} = \int\limits_{P_n^h}^{P_{n'}^h} \sigma^{-1} v_{n'}(\xi)\, d\xi, \tag{18}$$

where $v_{n'}$ is the projection of $\vec{v}$ on $d_{n,n'}$ and $v_{n,n'}$ is the value of $v_{n'}$ in the middle of this segment.

Using simple approximations of (17), we have

$$\sum_{n'} S_{n,n'} v_{n,n'} \cong V_n f_n, \quad n \in \overline{\Omega}^h / \Gamma^{e,D} = \widetilde{\Omega}^h, \tag{19}$$

$$\sigma_{n,n'}(u_n - u_{n'}) \cong d_{n,n'} v_{n,n'}, \quad \sigma_{n,n'} = \left[\int\limits_{P_n^h}^{P_{n'}^h} \sigma^{-1}(\xi)\, d\xi \right]^{-1}. \tag{20}$$

Here V_n, $S_{n,n'}$, $d_{n,n'}$ mean the values of the corresponding volume, area, and length. After excluding $v_{n,n'}$ from (19), obtain the SLAE

$$(Au^h)_n \equiv \sum_{n'} \frac{\sigma_{n,n'}}{d_{n,n'}} S_{n,n'}(u_n - u_{n'}) = V_n f_n, \quad n \in \widetilde{\Omega}^h. \tag{21}$$

It is supposed in (21) that if $P_{n'} \in \Gamma^{e,D}$ (the Dirichlet node), then we set $u_{n'} = g(P_{n'})$, and the corresponding term is replaced from the left- to the right-hand side. Also, if $P_n \in \Gamma^{e,N}$ and $S_{n,n'} = V_n \cap \Gamma^{e,N}$, then from the sequence of equation (3) we have

$$\sigma_n \alpha_n u_n + \sigma_n u_{n,n'} = \sigma_n \beta_n. \tag{22}$$

So, take into account this boundary condition by adding the terms $S_{n,n'}\sigma_n\alpha_n u_n$ and $S_{n,n'}\sigma_n\beta_n$ to the left- and the right-hand sides of (22), respectively.

Now, let ω_p^e be the set of N_p mesh nodes P_n which are the vertices of the finite element E_p. Each element can be divided into a set of sub-elements

$$E_{p,n} = E_p \cap V_n, \quad n \in \omega_p^e.$$

Let us denote by $S_{p,n',n''}$ the joint boundary segment of the sub-elements $E_{p,n'}, E_{p,n''}$, and by $S_{p,n'} = \bigcup_{n''} S_{p,n',n''}$ — the union of the boundary segments, corresponding to the node $P_{n'}$. If we define the "local flux" vector $\bar{v}^{(p)}$ of N_p, whose components are approximations of the integrals

$$v_n^{(p)} = \int\limits_{S_{p,n'}} v_{n,n'}\, ds \cong \sum_{n' \in \omega_p^e} a_{n,n'}^{(p)} u_{n'}, \tag{23}$$

and, also, define the local vector $\bar{u}^{(p)} = \{u_n^{(p)},\ n \in \omega_p^e\}$ of the same order, the following linear relation can be written down:

$$\bar{v}^{(p)} = A^{(p)} \bar{u}^{(p)}. \tag{24}$$

Here the square matrix $A^{(p)} = \{a_{n,n'}^{(p)}\}$ of order N_p is called a local balance matric. The global matrix A of system (21) is formed by means of the assembling procedure, see [2], for details.

2.3. Iterative solution of SLAE. The obtained algebraic system

$$Au = f \tag{25}$$

has a Stiltjies (symmetric, positive definite, and positive type) matrix. For solving this equation, we use a preconditioned, by explicit incomplete two-parametrized factorization, conjugate gradient method, see [9].

Define the explicit (i.e., non-block, or point-wise) preconditioning matrix as

$$B = (G-L)G^{-1}(G-U), \quad G = \frac{1}{\omega}D-\theta S, \quad S\,e = \left(\frac{1-\omega}{\omega}D+LG^{-1}\right)e, \tag{26}$$

where ω and θ are relaxation and compensation parameters, $e = \{1\}$ is a vector with unit entries, S and G are diagonal matrices. The preconditioner B provides the row sum criteria for $\theta = 1$, or a compensation principle, $Be = Ae$.

Because G is s.p.d.-matrix, system (25) is transformed to the equivalent preconditioned system

$$\tilde{A}\tilde{u} = \tilde{f}, \tag{27}$$

$$\begin{aligned}
&\tilde{A} = G^{1/2}(G-L)^{-1}A(G-U)^{-1}G^{1/2} \\
&\quad = (I-\tilde{L})^{-1} + (I-\tilde{U})^{-1} - (I-\tilde{L})^{-1}(2I-\tilde{D})(I-\tilde{U})^{-1}, \\
&\tilde{L} = G^{-1/2}L\,G^{-1/2}, \quad \tilde{U} = G^{-1/2}U\,G^{-1/2}, \quad \tilde{D} = G^{-1/2}D\,G^{-1/2}, \\
&\tilde{u} = (I-\tilde{U})G^{1/2}u, \quad \tilde{f} = (I-\tilde{L})^{-1}G^{-1/2}f.
\end{aligned}$$

An important idea of the above transformation consists in the spectral condition number property (for s.p.d.-matrices B, A)

$$\mathrm{cond}(\tilde{A}) = \mathrm{cond}(B^{-1}A) \tag{28}$$

and in a simple implementation of the matrix-vector multiplication:

$$\tilde{A}p = q + (I-\tilde{L})^{-1}[p - (2\,I-\tilde{D})q], \quad q = (I-\tilde{U})^{-1}p, \tag{29}$$

which demands approximately the same number of arithmetical operations as matrix-vector product Ap.

The classical preconditioned conjugate gradient method for s.p.d.-matrix $\tilde{A}$, in terms of system (27), can be written down as follows (let us call it EXIFCG):

$$\tilde{r}^0 = \tilde{f} - \tilde{A}\tilde{u}^0, \quad p^0 = \tilde{r}^0,$$
$$\tilde{u}^{n+1} = \tilde{u}^n + \alpha_n p^n, \quad \tilde{r}^{n+1} = \tilde{r}^n - \alpha_n \tilde{A} p^n, \quad \alpha_n = \frac{(\tilde{r}^n, \tilde{r}^n)}{(\tilde{A}p^n, p^n)}, \tag{30}$$
$$p^{n+1} = \tilde{r}^{n+1} + \beta_n p^n, \quad \beta_n = \frac{(\tilde{r}^{n+1}, \tilde{r}^{n+1})}{(\tilde{r}^n, \tilde{r}^n)}, \quad n = 0, 1, 2, \ldots$$

This iterative process provides at each n the minimization of the functional $\varphi_n = (\tilde{A}^{-1}\tilde{r}^n, \tilde{r}^n)$. The necessary number of iteration, for satisfying the condition $\varphi_n/\varphi_0 \le \varepsilon < 1$, is estimated by the inequality

$$n(\varepsilon) \le 1 + \frac{1}{2}\Big|\ln\frac{\varepsilon}{2}\Big|\sqrt{\operatorname{cond}\tilde{A}}, \tag{31}$$

where the condition number of preconditioned matrix $\tilde{A}$ is defined in (28). But, because the values φ_n are not known when implementing formulas (30), the stopping criteria in iterations is used as

$$[(\tilde{r}^n, \tilde{r}^n)/(\tilde{r}^0, \tilde{r}^0)]^{1/2} \le \varepsilon. \tag{32}$$

3. Numerical results

We present and discuss the results of experiments for the solution to equation (1) on a non-structured grid. The first example is the model Dirichlet boundary value problem for the subdomain Ω_2 (a parallelepiped with a cylindrical hole; $\sigma = 1$, $H = 4$, $H^z = 15$, $R = 1$), described in Figure 1. The exact solution and the boundary condition were chosen as $u = \ln\sqrt{x^2 + y^2}$. In Table 1, the maximal errors δ of the obtained solutions and numbers of iterations are given for $\varepsilon = 10^{-6}$ and $\varepsilon = 10^{-8}$ for three types of embedded grids: coarse Ω_c^h, middle Ω_m^h, and fine Ω_f^h. Here N means the number of mesh points.

Table 1. Numerical results for Problem 1

Subdomain	N	$\delta(\varepsilon = 10^{-6})$	n $(\varepsilon = 10^{-6})$	δ $(\varepsilon = 10^{-8})$	n $(\varepsilon = 10^{-8})$
Ω_c^h	2560	$1.657 \cdot 10^{-3}$	14	$1.657 \cdot 10^{-3}$	18
Ω_m^h	17856	$4.300 \cdot 10^{-4}$	17	$4.298 \cdot 10^{-4}$	22
Ω_f^h	132736	$1.121 \cdot 10^{-4}$	25	$1.119 \cdot 10^{-4}$	33

As can be seen from this table, the order of accuracy of the grid solution is $O(h^2)$, where h is a characteristic mesh step. The number of iteration is approximately proportional to $h^{-1/2}$. So, the efficiency of approach used is the same, as for a uniform parallelepiped grid (see numerical results in [9, 10]).

The second example is closer to practice and presents two vertical cylinders which are placed into horizontal layer media with a piecewise constant $\sigma(\vec{x})$ (Figure 3).

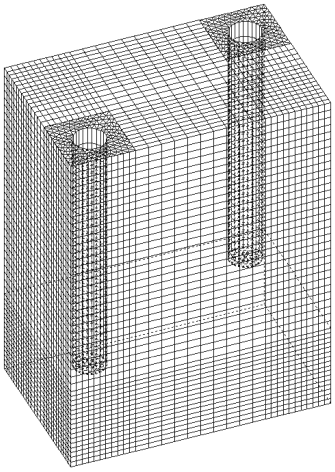

Figure 3. Computational grid for Problem 2

The computational domain is a parallelepiped $\Omega = [0,16]\times[0,10]\times[0,20]$ including three subdomains

$$\Omega_1 = [0,16]\times[0,10]\times[0,5],$$
$$\Omega_2 = [0,4]\times[0,4]\times[5,20],$$
$$\Omega_3 = [12,16]\times[6,10]\times[5,20]$$

and two cylindrical holes

$$\Omega_4 = \{(x-2)^2+(y-2)^2 \le 1,\ 5 \le z \le 20\},$$
$$\Omega_5 = \{(x-14)^2+(y-8)^2 \le 1,\ 5 \le z \le 20\}.$$

The values of the coefficient in (1) are equal to $\sigma = 1$, except subdomains: in Ω_1, $\sigma = 0.1$; in $(\Omega_2\setminus\Omega_4)\cup(\Omega_3\setminus\Omega_5)$, $\sigma = 10$, and in $\Omega_4\cup\Omega_5$, $\sigma = 0$ (the external subdomain).

The boundary conditions are $u|_{\Gamma_4} = u|_{\Gamma_5} = 0$ and $\dfrac{\partial u}{\partial n} = 0$ at the external faces of the parallelepiped Ω. Numerical results on the coarse, middle and fine embedded grids at a few different points are presented in Table 2.

Table 2. Numerical results for Problem 2

	P_1	P_2	P_3	P_4	P_5
Ω_c, $N = 37492$, $n = 477$	$2.9191\cdot10^{-2}$	0.66883	4.3264	4.9709	4.5195
Ω_m, $N = 284330$, $n = 731$	$2.9643\cdot10^{-2}$	0.67259	4.3202	4.9703	4.5181
Ω_f, $N = 2212804$, $n = 860$	$2.9787\cdot10^{-2}$	0.67400	4.3174	4.9702	4.5185
$\|u_c - u_m\|$	$452\cdot10^{-2}$	$376\cdot10^{-5}$	$62\cdot10^{-4}$	$6\cdot10^{-4}$	$6\cdot10^{-4}$
$\|u_m - u_f\|$	$144\cdot10^{-6}$	$141\cdot10^{-4}$	$26\cdot10^{-4}$	$1\cdot10^{-4}$	$4\cdot10^{-4}$

Because this BVP does not have analytical solution, we analyze the differences of solutions on various grids. As can be seen, the convergence of the grid solution obtained is close to the second order. The number of iterations is acceptable and can be estimated as $O(h^{-1/2})$.

References

[1] Axelsson O., Barker V.A. Finite Element Solution of Boundary Value Problems. Theory and Computations. — New York: Academic Press, 1984.

[2] Il'in V.P. Finite Difference and Finite Volume Methods for Elliptic Equations. — Novosibirsk: ICM&MG, 2001 (In Russian).

[3] Kozlovsky G. Solving partial differential equations using recursive grids // Appl. Num. Math. — 1994. — Vol. 14. — P. 165–181.

[4] Liseikin V.D. Grid Generation Methods. — Berlin: Springer, 1999.

[5] Il'in V.P. Computational informational technologies of mathematical modeling // Avtometriya. — 2000. — No. 1. — P. 3–13.

[6] Il'in V.P. Geometrical and functional modeling in mathematical physics problems // Computational Technologies. – Novosibirsk, 2001. — Vol. 6, No. 2. — P. 315–321 (In Russian).

[7] Pissanetzky S. Sparse Matrix Technology. — New York: Academic Press, 1984.

[8] Il'in V.P. On the mixed finite volume methods // Joint issue of Comput. Technologies. Part 2. — Novosibirsk; Almaaty, 2004. — Vol. 9, No. 3. — P. 245–253 (In Russian).

[9] Il'in V.P., Itskovich E.A. Two explicit incomplete factorization methods // NCC Bulletin. Series Numerical Analysis. — Novosibirsk: NCC Publisher, 2002. — Issue 11. — P. 51–60.

[10] Il'in V.P. Incomplete Factorization Methods. — Singapore: World Sci. Publ., 1992.